

Azocoupling products VI.¹ The sensitivity to external factors of the UV–vis absorption spectra of the azocoupling product between 1-(4-hydroxy-6-methyl-pyrimidin-2-yl)-3-methylpyrazolin-5-one and 4-(*N,N*-dimethyl) aminobenzenediazonium salt

Ioan Panea, Mirela Pelea*, Ioan A. Silberg

Department of Organic Chemistry, “Babeş-Bolyai” University, Arany Janos 11, RO, 400028 Cluj Napoca, Romania

Received 18 May 2005; received in revised form 12 January 2006; accepted 16 January 2006

Available online 11 April 2006

Abstract

The pH-, water content-, sample concentration-, temperature- and time-dependences of the UV–vis spectra of the potentially tautomeric azocoupling product **1** in (aqueous) ethanol solutions have been systematically investigated. On the basis of pH-dependence were determined the pK_a' values corresponding to three interconnected acid–base equilibria $2b \rightleftharpoons 1a \rightleftharpoons 3b \rightleftharpoons 4b$ that originate from **1**. The four species **1a**, **2b**, **3b**, **4b** involved in these equilibria are characterized on the basis of their different visible absorption bands. The hydrazone structure **1a** of the initial species is supported by the ¹H and ¹³C NMR data. The dependence of the UV–vis spectra of (aqueous) ethanol solution of **1** upon the water content, dye concentration, temperature or time seems to be due firstly to the acid–base equilibrium $1a \rightleftharpoons 3b$. However, some irregularities in these dependences might be interpreted as being caused by eventual superimposition upon the acid–base equilibrium $1a \rightleftharpoons 3b$ of the azo–hydrazone (e.g. $1a \rightleftharpoons 1b$) and/or aggregation equilibrium. By the time dependence has been observed practically a kind of oscillation of the position of the present equilibrium that is very difficult to explain.

© 2006 Elsevier Ltd. All rights reserved.

Keywords: Azocoupling product; Effect of pH; Water content; Sample concentration; Temperature and time on UV–vis spectra

1. Introduction

The compound **1** is an azocoupling product that might appear [1–3] in more azo- and hydrazone-tautomeric forms (e.g. **1a**, **1b**). However, it must be underlined that for the azocoupling products of the 1-aryl- or 1-hetaryl-3-methylpyrazolin-5-one – to which belongs also the compound **1** which forms the object of this study – most of the published papers [4–13] sustain the practical presence of only the hydrazone tautomers. Correspondingly, the ¹H NMR spectrum of

1 has been compatible even with hydrazone tautomer structure **1a** [3].

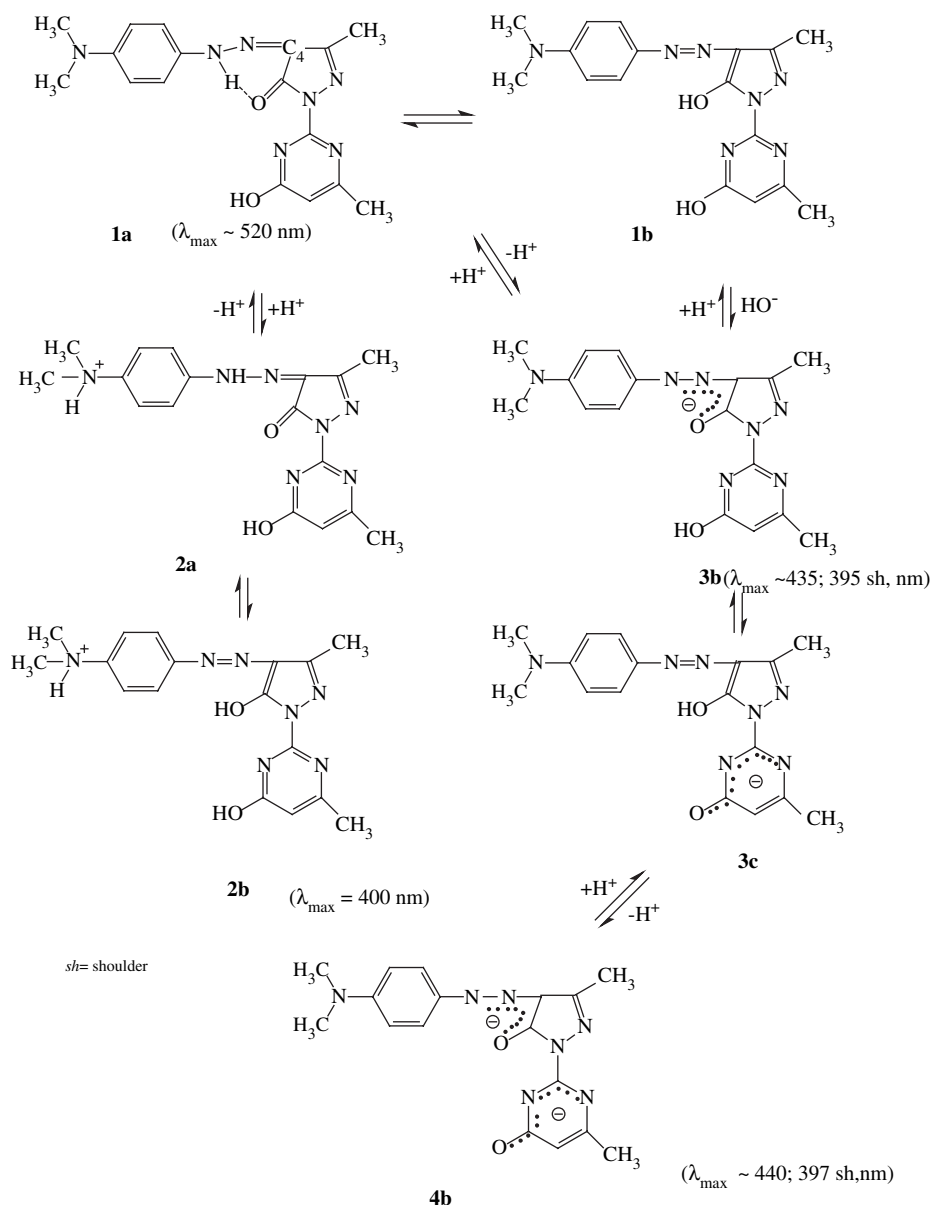
But owing the great sensitivity of the visible absorption spectrum of **1** to solvent nature and to acid, alkali or water addition, in some of its solutions,[3] the involvement of the hydrazone tautomer **1a** in interconnected azo–hydrazone was suggested (e.g. $1a \rightleftharpoons 1b$) and acid–base ($1a \rightleftharpoons 2b$, $1a \rightleftharpoons 3b$, $3b \rightleftharpoons 4b$) equilibria (Scheme 1).

In order to explain, otherwise, such a sensitivity to various experimental factors of the UV–vis spectra of many other dyes [14–16], but firstly of those able of azo–hydrazone tautomerism [9,10,17–32] different interconnected equilibria were also admitted [14,18,19b,22,25–28,30–32]: acid–base with aggregation [14], acid–base with azo–hydrazone [22,26,28,30–32], acid–base with azo–hydrazone and

* Corresponding author. Tel.: +40 264591998; fax: +40 264590818.

E-mail address: mpelea@chem.ubbcluj.ro (M. Pelea).

¹ Part V, see reference [32].



Scheme 1. Some of the interconnected azo-hydrazone and acid–base equilibria to which the dye **1** might participate.

aggregation [18,27b], azo–hydrazone with aggregation [19b,25,27b]. There are, however, authors who have adopted as explanation for such a sensitivity only one type of equilibria: acid–base [9,10,15,16,20,23,24] or azo–hydrazone [17,19a,21,29] or monomer–dimer [25b]. The above explanations have been formulated especially on the basis of a systematic study of the dependence of the UV–vis absorption spectra as a function of various factors: pH [9,10,14–16,18,20,22–24,26–28,32], solvents [7,17–21,25a,26b,28,30–32], acid [20,28,30–32], alkali [28,30–32], water [7,19a,21,32] or surfactants [27b] addition, temperature [19b,20,21a,25,29], time [27a,32], and dye concentration [18,20,25,27a,32].

Therefore, with the object to ascertain as accurately as possible, the cause of the sensitivity to experimental factors of the UV–vis spectra of the solutions of **1**, in this work we set

ourselves as a task such a systematic UV–vis study. For this purpose, the data obtained in the previous paper [3] concerning the dependence of UV–vis spectra of **1** as a function of solvents and acid or alkali addition to the ethanol or methanol solutions, respectively, have been completed with those on the dependence of the UV–vis spectra of the (aqueous) ethanol solutions of **1** against pH, water content, dye concentration, temperature and time, respectively. Supplementary, is made also a full assignment of the signals from ^1H and ^{13}C NMR spectra of **1**. Thus we hope to determine also the existing forms of **1** in the examined conditions. Also, the pH-dependence of the above UV–vis spectra of **1** was used to determine the $\text{p}K_a'$ values of **1**. The studied species, that may appear in more tautomeric forms, are indicated generally as **1**, **2**, **3**, **4**, but as **1a**, **1b**, **2a**, **2b**, etc., for a definite tautomer.

2. Results and discussion

2.1. NMR spectra of **1** in CDCl₃

The assignment of the signals from the ¹H and ¹³C NMR spectra of **1** in CDCl₃ is presented in Tables 1 and 2. The analysis of the ¹H NMR spectrum of **1** has been facilitated by great diagnosis value of the most intensive signal of this spectrum, namely that which is due to the six protons corresponding to the N(CH₃)₂ group. On this basis it has been possible to find the total number of hydrogen atoms in the molecule **1** and the number of hydrogen atoms corresponding to each signal and to each type of hydrogen atoms, respectively. As expected these numbers are compatible with any tautomeric forms of **1** (e.g. **1a**, **1b**). As in the ¹H NMR spectrum of **1** appears only one signal corresponding to the protons of N(CH₃)₂ group it may be appreciated that in CDCl₃ solution **1** is detected formally only as a single species or if there are more tautomeric (or of another type) species these should be in a rapid equilibrium. On the other hand, the presence in the ¹H NMR spectrum of **1** of a very low field signal (13.55 ppm) supports the hydrazone tautomer structure **1a** for the detected species because for the other pyrazolin-5-one azocoupling products such a signal was argued to be characteristic just for the hydrazone NH proton [3,4,7–9,12,13,30,31]. However, it is noteworthy that the chemical shift (3.04 ppm) of the hydrogen atoms present in the N(CH₃)₂ group of **1** is very similar to that found (3.1 ppm) for the same group bounded at one end of the polymethine chain in some merocyanine dyes (cf. [34]). This, in spite of the fact that the type of extensive conjugation characteristic for merocyanine [35] – that explains the deshielding of the N(CH₃)₂ group protons of these – may not involve formally the N(CH₃)₂ group in the case of **1a** (see formulae **1a**).

In exchange the ¹³C-chemical shifts for **1** (Table 2) are similar to those of the same types of carbon atoms present in other pyrazolin-5-one azocoupling products for which has been assigned a hydrazone structure [3,5,7,8,30]. Therefore on the

Table 2

The ¹³C-chemical shifts of **1**, corresponding to hydrazone structure **1c**^a, of 1-phenyl-3-methyl-4-phenyl-hydrazonepyrazolin-5-one and of the 1-(4-hydroxy-6-methyl-pyrimidinil-2-yl) analogue^b of the last

The position of C-atoms	¹³ C-chemical shifts δ (ppm) for the compounds			
	1 (1c)	1-Ph-3-Me-4-Ph-hydrazonepyrazolin-5-one	Analogue of 1c unsubstituted in the benzene ring	Calculated ¹³ C-chemical shifts for the “a–d” C-atoms in 1
3	<i>147.1</i>	<i>148.4</i>	<i>146.6</i>	
4	<i>124.0</i>	<i>128.4</i>	<i>125.8</i>	
5	<i>159.5</i>	<i>157.7</i>	<i>159.0</i>	
1' (3')	—	118.4	—	
2'	<i>161.5</i>	138.0	<i>161.3</i>	
4'	<i>165.9</i>	128.8	<i>165.8</i>	
5'	<i>109.2</i>	125.0	<i>109.5</i>	
6'	<i>152.1</i>	128.8	<i>152.5</i>	
a	<i>150.1</i>	<i>125.7</i>	<i>127.5</i>	<i>150.3^c</i>
b	<i>112.6</i>	<i>129.6</i>	<i>129.9</i>	<i>114.2^c</i>
c	<i>118.4</i>	<i>115.7</i>	<i>116.7</i>	<i>117.5^c</i>
d	<i>129.8</i>	<i>141.1</i>	<i>140.4</i>	<i>128.6^c</i>
3-CH ₃	<i>12.1</i>	<i>11.7</i>	<i>12.1</i>	
6'-CH ₃	24.6	—	24.6	
N(CH ₃) ₂	40.4	—	—	

The data for 1-Ph-3-Me-4-Ph-hydrazonepyrazolin-5-one are from references [5a,8].

The similar italicized values are to be compared.

^a See the structure of **1c** in Table 1.

^b This corresponds to the structure of **1c** unsubstituted in the benzene ring.

^c These are calculated from the corresponding values of the unsubstituted analogue in benzene ring – presented in preceding column – using the increments of the N(CH₃)₂ substituent in *para*-position [33].

basis of NMR study of **1** it is concluded (cf. [3]) that in CDCl₃ solution the structure of **1** corresponds to **1a**.

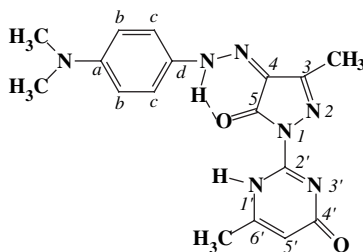
2.2. UV–vis spectroscopic study

2.2.1. Preliminary remarks

As we have shown previously [3] the dye **1** has practically the same UV–vis spectrum with only one intense and

Table 1

The ¹H NMR data^a of **1** corresponding to the hydrazone structure **1c**



1c

Protons of the group							
C(6')–CH ₃	C(3)–CH ₃	N(CH ₃)	C(5')–H	C(b)–H	C(c)–H	N(1)–H	Hydrazone NH
2.36; s; 3H	2.41; s; 3H	3.04; s; 6H	6.08; s; 1H	6.73; d; 2H; 8.2	7.39; d; 2H; 8.2	11.4; s; 1H	13.55; s; 1H

^a There are given the chemical shift – δ (ppm), the multiplicity (s – singlet; d – doublet), the number of protons and the coupling constant – J (Hz).

relatively narrow absorption band in visible ($\lambda_{\max} \sim 520$ nm) – in CDCl_3 , benzene, CCl_4 , dioxane, dimethylsulfoxide, anhydrous pyridine, and acidified ethanol or methanol. On this basis and because for **1** in CDCl_3 has been assigned a hydrazone structure **1a** (see Section 2.1) the same structure should be present in all above solutions. In exchange, the visible spectra in diluted ($\sim 10^{-5}$ mol L^{-1}) neutral ethanol or methanol solutions of **1** present usually three absorption bands ($\lambda_{\max} \sim 520, 435, 395$ nm), even if some of these appear only as shoulder (Fig. 1, curve 1). But these spectra with three bands are converted by the addition of a small quantity of acid ($[\text{HCl}] = 2 \times 10^{-4}$ mol L^{-1}) into spectra with only one band in visible ($\lambda_{\max} \sim 520$ nm, Fig. 1, curve 2) which corresponds to the spectrum of **1** in CDCl_3 that has been assigned to the hydrazone structure **1a** (see above). In other words, by the addition of small amounts of acid the disappearance of the bands from $\sim 435, 395$ nm takes place on account of the corresponding increase in the band at ~ 520 nm (Fig. 1, curve 2). Approximately the same effect is also determined by the addition of much water to the ethanol solution of **1** (Fig. 1, curve 3).

On the other hand, the addition of more acid (up to $[\text{HCl}] = 10^{-1}$ mol L^{-1}) to the above acidified ethanol solution of **1** (Fig. 1, curve 2) converts the spectrum with only one visible band of this ~ 520 nm into a spectrum with another unique visible band (Fig. 1, curve 4). But in this last case the single visible band is located at the lowest wavelength in visible ($\lambda_{\max} \sim 400$ nm). In exchange, if the added quantity of acid to the solutions having the absorption curves 1 or 2 in Fig. 1 is intermediate between the two above mentioned, there takes place (Fig. 1, curve 5): (i) a decrease in the longest wavelength band at 520 nm, (ii) the disappearance of the band at ~ 435 nm – in the case of diluted neutral ethanol

solution – and (iii) an increase in the band at 400 nm. The greater quantity of acid leads in fact to the disappearance also of the longest wavelength band (~ 520 nm) on account of the corresponding increase in the band at 400 nm. Also, the addition of KOH to ethanol or methanol solutions of **1** influences the visible spectra of these. A small quantity of KOH only diminishes (Fig. 1, curve 6) the longest wavelength band (520 nm) whilst more KOH determines its disappearance (Fig. 1, curve 7) on account of the corresponding increase in two bands of lower wavelength (435, 395 nm). The above-discussed behaviors are compatible (cf. [3]) with the involvement of the assigned hydrazone tautomer **1a** ($\lambda_{\max} \sim 520$ nm) in different equilibria (cf. Scheme 1), especially in the examined (aqueous) ethanol solutions.

With the aim to ascertain as accurate as possible these equilibria, further is examined the influence of the pH, of the water content, of the dye concentration, of the temperature and of the time on the spectra of **1** in (aqueous) ethanol.

2.2.2. Influence of pH. The determination of pK_a' values

The pH has a very great influence on the UV–vis spectra of **1** in aqueous ethanol solutions (Fig. 2). The absorption curves of the isomolar solutions of **1** in aqueous ethanol present different isosbestic points as a function of pH' range. However, by the examination of the UV–vis spectra in certain pH' ranges, namely: 1.8–5.6 (Fig. 3), 5.6–10.6 (Fig. 4), 10.6–12.6 (Fig. 5), respectively, the absorption curves present the same sharp isosbestic points in a certain pH' range even if these are different in the three mentioned ranges.

The plot of absorbance vs. pH' at the analytical wavelength (520 nm) in each above delimited range has a sigmoidal form (e.g. Fig. 6). Such a form is characteristic for an acid–base equilibrium [22,23,32,36a]. By derivation of the sigmoidal curves (e.g. Fig. 7) were obtained the pK_a' values corresponding to the three above pH ranges: $\text{pK}_{a1}' = 3 \pm 0.03$, $\text{pK}_{a2}' = 7.06 \pm 0.03$, $\text{pK}_{a1}' = 11.31 \pm 0.03$. The first pK_a

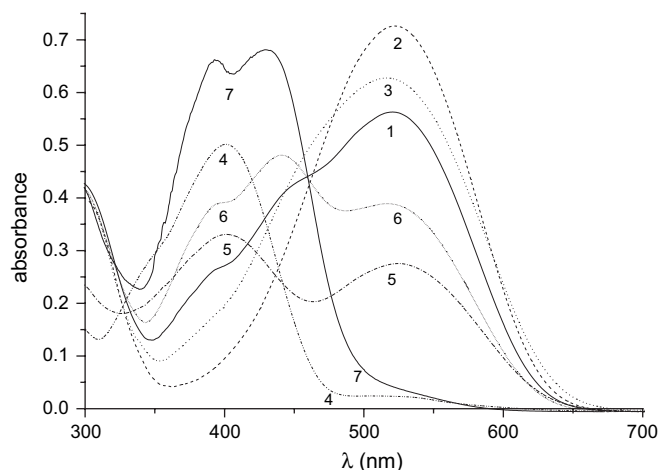


Fig. 1. The spectra of **1** in ethanol solutions with different additions of acid, alkali or water. 1 – the initial ethanol solution of **1** ($c = 2.83 \times 10^{-5}$ mol L^{-1}); 2 – the initial (1) solution of **1** after addition of low quantity of HCl (to $\sim 10^{-4}$ mol L^{-1}); 3 – the 50% ethanol–water (v/v) solution of **1**; 4 – the initial (1) solution of **1** after addition of more HCl (to $\sim 10^{-1}$ mol L^{-1}); 5 – the initial (1) solution of **1** after addition of an intermediate quantity of HCl between those corresponding to absorption curves 2 and 4; 6 – the initial (1) solution of **1** after addition of low quantity of KOH (to $\sim 3 \times 10^{-5}$ mol L^{-1}); 7 – the initial (1) solution of **1** after addition of more KOH (to $\sim 10^{-1}$ mol L^{-1}).

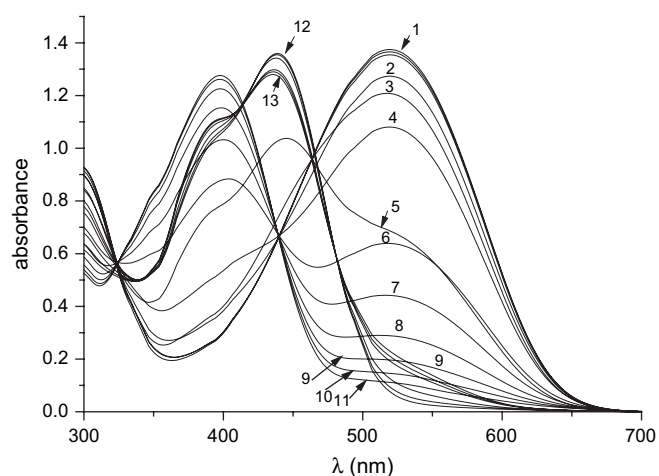


Fig. 2. The pH' dependence of the spectra of the isomolar solutions of **1** ($c = 2.97 \times 10^{-5}$ mol L^{-1}) in ethanol–water (1 v/1 v) at ionic strength of 0.01 mol L^{-1} KCl at 25 °C. For some curves are indicated the pH' values: 1 – 4.83; 2 – 4.01; 3 – 6.32; 4 – 3.58; 5 – 7.36; 6 – 2.94; 7 – 2.73; 8 – 2.45; 9 – 2.23; 10 – 2.03; 11 – 1.79; 12 – 12.08; 13 – 9.55.

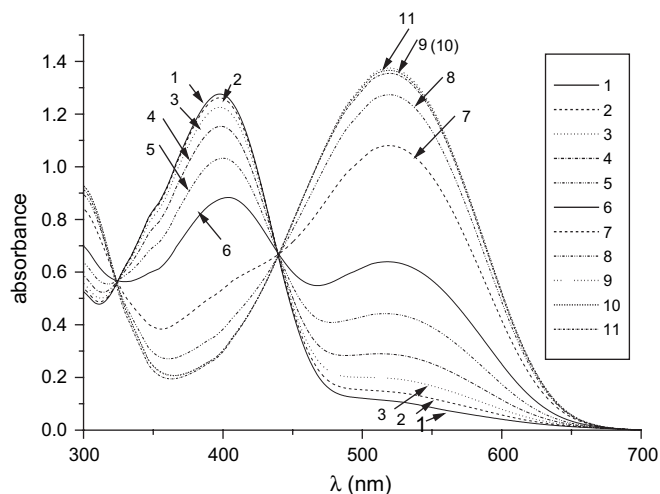


Fig. 3. The pH' dependence of the spectra of the isomolar solutions of **1** ($c = 2.97 \times 10^{-5} \text{ mol L}^{-1}$) in ethanol–water (1 v/1 v) at ionic strength of 0.01 mol L^{-1} KCl at 25°C . For some curves are indicated the pH values: 1 – 1.79; 2 – 2.03; 3 – 2.23; 4 – 2.45; 5 – 2.73; 6 – 2.94; 7 – 3.53; 8 – 4.01; 9 – 4.83; 10 – 5.06; 11 – 5.60.

($\text{p}K_{\text{a}1}'$) seems to correspond (cf. [10,18,22,26a,36b]) to the protonation equilibrium of the dye **1** ($1 + \text{H}^+ \rightleftharpoons 2\text{b}$), while the $\text{p}K_{\text{a}2}'$ and $\text{p}K_{\text{a}3}'$ should correspond (cf. [9,16,18,20,21a,22–24,26,27b,28,32,36–40]) to the deprotonation equilibria of **1** ($1 + \text{HO}^- \rightleftharpoons 3\text{b}$ and $3\text{b} + \text{HO}^- \rightleftharpoons 4\text{b}$, respectively, see Scheme 1). On the other hand, the presence of the well-defined isobestic points for the absorption curves in each above delimited pH range (Figs. 3–5) is compatible with the manifestation of acid–base equilibrium only between two species in each of the three above pH range. The three acid–base equilibria are interconnected because they have as origin the same compound **1**. Therefore, the total number of the involved species should be four: the protonated form **2b** (or **2a**) ($\lambda_{\text{max}} \sim 400 \text{ nm}$), the initial species **1a** ($\lambda_{\text{max}} \sim 520 \text{ nm}$), the monodeprotonated species **3b** ($\lambda_{\text{max}} \sim 435$ and 395-sh nm)

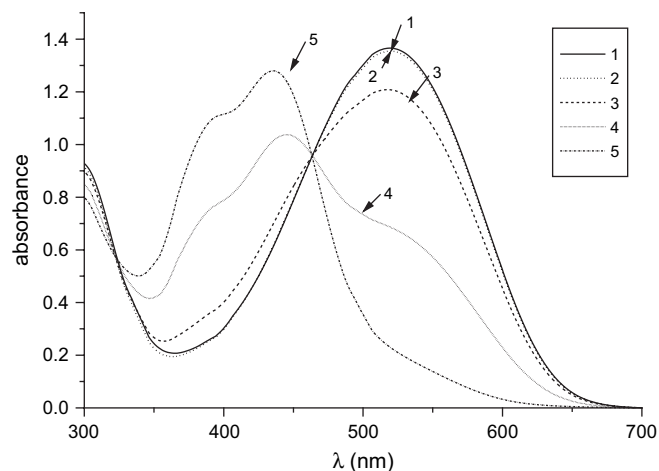


Fig. 4. The pH' dependence of the spectra of the isomolar solutions of **1** ($c = 2.97 \times 10^{-5} \text{ mol L}^{-1}$) in ethanol–water (1 v/1 v) at ionic strength of 0.01 mol L^{-1} KCl at 25°C , in the pH' range 5.6–10.55. 1 – 5.60; 2 – 6.32; 3 – 7.36; 4 – 9.55; 5 – 10.55.

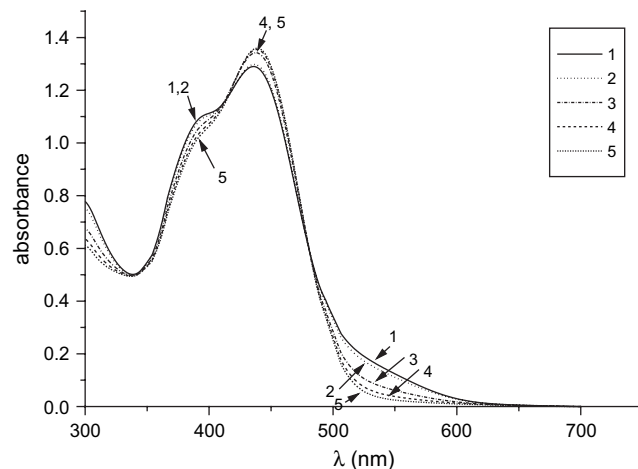


Fig. 5. The pH' dependence of the spectra of the isomolar solutions of **1** ($c = 2.97 \times 10^{-5} \text{ mol L}^{-1}$) in ethanol–water (1 v/1 v) at ionic strength of 0.01 mol L^{-1} KCl at 25°C , in the pH' range 10.55–12.58. 1 – 10.55; 2 – 10.91; 3 – 11.64; 4 – 12.08; 5 – 12.58.

and the double deprotonated species **4b** ($\lambda_{\text{max}} \sim 440$ and 397-sh nm). As has been shown (see Section 2.1) the initial species has been detected by NMR only as hydrazone tautomer **1a**. The fact that the protonation of the initial species (Fig. 1, curve 4, $[\text{HCl}] = 10^{-1} \text{ mol L}^{-1}$) causes a very large hypsochromic shift of the longest wavelength band (from 520 to 400 nm) suggests a major change of the chromophore system, e.g. from **1a** to the hydroxyazo tautomer form **2b** of the protonated species of **1** (see also Fig. 3). Such a transformation by protonation of the hydrazone tautomers has been ascribed [10] also in the case of other pyrazolin-5-one azocoupling products. Also, monodeprotonated species of **1** exhibits a large hypsochromic shift of the longest wavelength band relative to the one of the initial species (from 520 to about 435 and 395-sh nm, see Figs. 1 and 4). Therefore we assign for this a common anion structure having principally an azonature **3b**, as have been given also for the corresponding anion arising from other azo-coupling products capable of azo–hydrazone tautomerism [20,26,32,36b–39]. However, it is noteworthy that the initial species **1**, its monoprotonated species **2** and its monodeprotonated species **3** may appear in more tautomeric forms

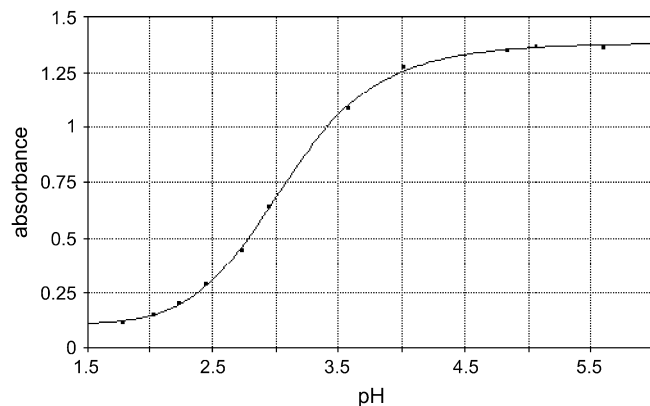


Fig. 6. The plot absorbance vs. pH' corresponding to the pH' range 1.79–5.6, respectively, to the $\text{p}K_{\text{a}1}'$ determination of the dye **1**.

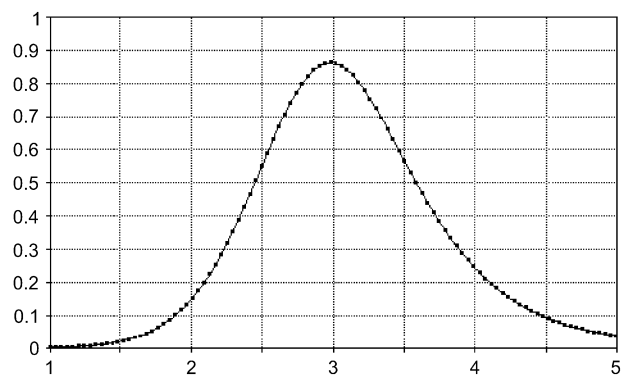


Fig. 7. The first derivative for the plot from Fig. 6 that gives the pK_{a1}' value.

(e.g. $1a \rightleftharpoons 1b$, $2a \rightleftharpoons 2b$, $3a \rightleftharpoons 3c$). In exchange, the twice deprotonated species of **1** appear only as delocalized dianion that should have principally also an azostructure **4b**. The great similarity between the UV–vis spectra of the twice deprotonated **4b** and monodeprotonated **3b** species (Fig. 5) – for which has been assigned above an azostructure – supports this assignment. As a conclusion of the study of the pH' dependence of the UV–vis spectra and of the pK_{a1}' determination for **1** it must be underlined that such obtained data undoubtedly prove the involvement of **1** in acid–base equilibria. Consequently, an explanation of the great sensitivity of the UV–vis spectra of the (aqueous) ethanol solutions of **1** to different experimental factors, but firstly to acid or base presence, should be even the manifestation in these conditions of the acid–base equilibria.

2.2.3. The effect of water content in ethanol solutions

The UV–vis absorption curves of isomolar solutions of **1** in ethanol with different water content (0–50%) are presented in Fig. 8. The modification of the composition of the solvent from absolute ethanol (curve 1) to 50% (v/v) ethanol–water (curve 6) has approximately the same effect as the addition

of small quantity of acid ($[HCl] = 2 \times 10^{-4} \text{ mol L}^{-1}$) to the solution of **1** in absolute ethanol (compare the curves 2 and 3 from Fig. 1). On the other hand, the absorption curves from Fig. 8 are similar to some absorption curves from Fig. 4, curves that correspond to the first deprotonation equilibrium $1a \rightleftharpoons 3b$. Therefore, it may be appreciated that the water addition to the ethanol solution of **1** determines the shift of the equilibrium $1a \rightleftharpoons 3b$ towards **1a** (cf. [32]) because the water is a stronger acid than the ethanol. Hence the sensitivity to the water content of the ethanol solutions of **1** is caused apparently by the manifestation of the acid–base equilibrium $3b \rightleftharpoons 1a$. We mention that the UV–vis spectra of the 4-phenylazo-1-naphthol show a similar dependence upon the water content of ethanol as that exhibited in the case of **1**. But this dependence in the case of 4-phenylazo-1-naphthol has been ascribed to the azo–hydrazone tautomerism [7,19a,21].

2.2.4. The effect of dye **1** concentration in ethanol solutions

The UV–vis absorption curves in ethanol at different concentrations of **1** in the range 10^{-4} – $10^{-6} \text{ mol L}^{-1}$, keeping constant the value “ $c_D \times l$ ” (c_D = dye concentration, l = path length of the cell) are presented in Fig. 9. They are similar to some absorption curves from Fig. 8 that have been shown above (Section 2.2.3) to correspond apparently to the first deprotonation equilibrium $1a \rightleftharpoons 3b$. In accordance with such an equilibrium the decrease in the concentration (the dilution) shifts this towards deprotonated (or ionized) form **3b**. Otherwise such an interpretation of dye concentration effect has been given recently for other azocoupling products capable of azo–hydrazone tautomerism [20,28,32]. Consequently, we consider that also the sensitivity of the UV–vis spectra in ethanol towards the dye **1** concentration variation is caused very likely by acid–base equilibrium $1a \rightleftharpoons 3b$.

We mention, however, that a concentration dependence of the UV–vis absorption spectra similar to that shown by **1**

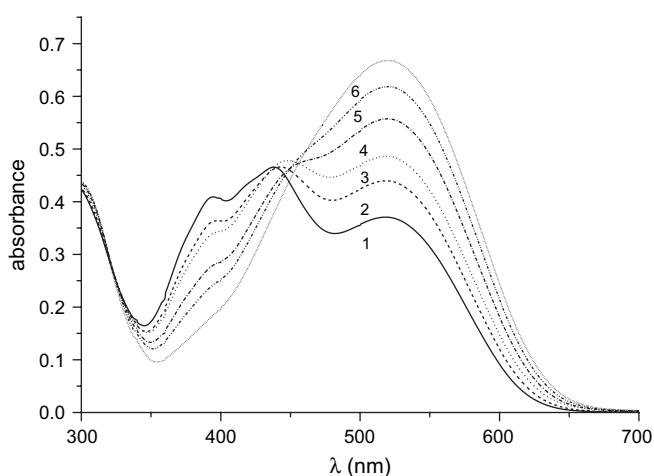


Fig. 8. The dependence of the spectra of the isomolar (aqueous) ethanol solutions of **1** ($c = 1.322 \times 10^{-5} \text{ mol L}^{-1}$) on the water content at 25 °C. 1 – Absolute ethanol solution; 2 – ethanol–water (9 v/1 v); 3 – ethanol–water (8 v/2 v); 4 – ethanol–water (7 v/3 v); 5 – ethanol–water (6 v/4 v); 6 – ethanol–water (1 v/1 v).

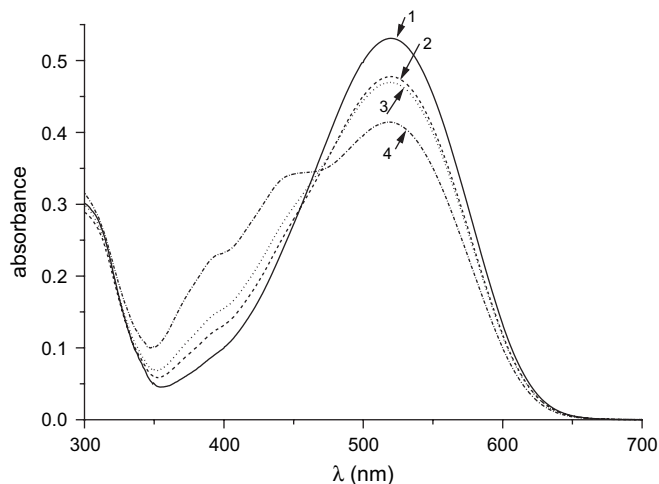


Fig. 9. The concentration dependence of the spectra of the dye **1** in absolute ethanol at 25 °C and constant product: $c_D \times l = 1.84 \times 10^{-5} \text{ mol L}^{-1}$. For each curve is given the dye concentration in mol L^{-1} and the path length of the cell in cm. 1 – 3.68×10^{-5} , 0.5; 2 – 1.84×10^{-5} , 1; 3 – 0.92×10^{-5} , 2; 4 – 3.68×10^{-6} , 5.

has been ascribed in the case of other azocoupling products to the aggregation [25b] or to the interconnected azo–hydrazone and aggregation equilibria [25a,27]. Concerning the alternative interpretations of the water content- or dye concentration- dependence it must be underlined that the UV–vis absorption curves of the isomolare solutions of **1** in ethanol with different water content (Fig. 8) as well as the absorption curves in ethanol at different concentrations of **1** and constant “ $c_D \times l$ ” value (Fig. 9) have given distorted isosbestic points. Such a situation might indicate that it is present as a non-simple ionization step (cf. [27b,32]), that the ionization equilibrium $1a \rightleftharpoons 3b$ is connected with another equilibrium, e.g. by azo–hydrazone (cf. [3,18,22,26,27b,28,31,32,36b,37,39,40]) – or (and) aggregation (cf. [14,27b,18]) – equilibrium. This possibility is more probable as the UV–vis spectrum of the common anion **3b** with a principally azostructure is expected to be similar to that of the corresponding unde protonated hydroxy–azo tautomer **1b** because in the two mentioned species should be present practically similar azochromophores. On the other hand also the UV–vis spectrum of the initial unde protonated hydrazone tautomer **1a** is expected to be quite similar to that of its eventual dimer on the basis of such findings [25] in the case of other azocoupling products that have been detected principally [25a] as hydrazone tautomers. Therefore, in the above conditions it is very difficult to differentiate the equilibria that involve very probably more species with similar UV–vis absorption spectra.

2.2.5. The effect of temperature on the visible spectra of the ethanol solutions of **1**

The UV–vis absorption curves of **1** in ethanol solutions at different temperatures in the range 18–60 °C are presented in Figs. 10 and 11. The temperature dependence of the spectra of **1** differs as a function of the source (Primexchim or mixture Primexchim + Cristal – Bucharest) of absolute ethanol.

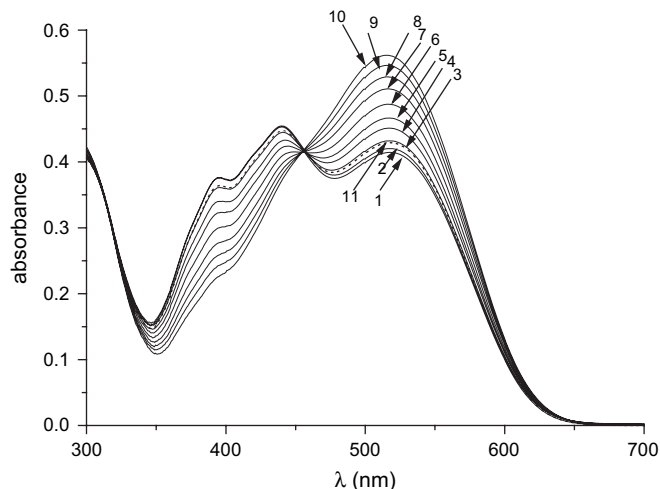


Fig. 10. The temperature dependence of the spectra of **1** ($c = 3.44 \times 10^{-5} \text{ mol L}^{-1}$) in absolute ethanol (mixture 87 v/13 v from the ethanol provided by Primexchim and Cristal (Bucharest), respectively). For each curve is given the measurement temperature in °C. 1 – 18; 2 – 21; 3 – 25; 4 – 30; 5 – 35; 6 – 40; 7 – 45; 8 – 50; 9 – 55; 10 – 60; 11 – after cooling to room temperature.

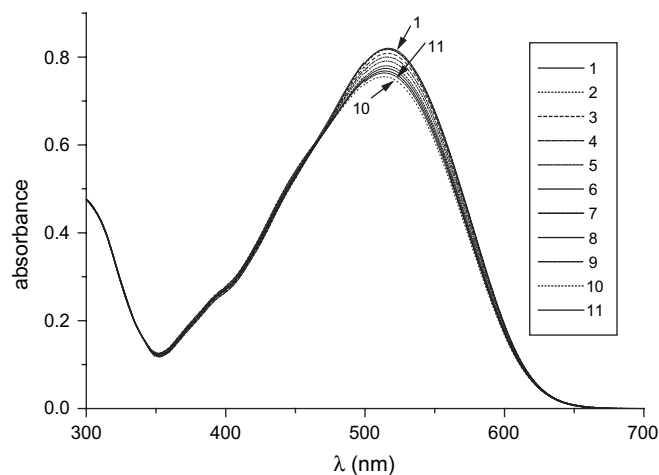


Fig. 11. The temperature dependence of the spectra of **1** ($c = 3.96 \times 10^{-5} \text{ mol L}^{-1}$) in absolute ethanol provided by Primexchim, Bucharest ($\text{pH}' = 7.90$). For each curve is given the measurement temperature in °C. 1 – 18; 2 – 20; 3 – 25; 4 – 30; 5 – 35; 6 – 40; 7 – 45; 8 – 50; 9 – 55; 10 – 60; 11 – after cooling to room temperature.

Namely, it is opposite for the two sorts of ethanol. We mention that the measured pH' of the ethanol from Primexchim was slightly lower ($\text{pH}' = 7.90$) than that from Cristal ($\text{pH}' = 8.90$). On the other hand the absorption curves from Figs. 10 and 11 are similar to some absorption curves from Figs. 8 and 9 that have been shown above (Sections 2.2.3 and 2.2.4) to correspond apparently to the acid–base equilibrium $1a \rightleftharpoons 3b$. On this basis we consider that also the temperature dependence of the spectra of **1** is caused by the same acid–base equilibrium $1a \rightleftharpoons 3b$. Otherwise such an opinion was formulated also concerning other potentially tautomeric azocoupling products [20,28] and it is known that the measured pH' changes with temperature [41].

However, it is noteworthy again that several authors ascribed the temperature dependence of the UV–vis spectra of some azocoupling products to the shift of their azo–hydrazone equilibrium [17b,21a,25a,29], while others [19b] considered the involvement of an aggregation equilibrium also. We should also take into consideration these two last possibilities for **1** especially because at slightly lower pH' (Fig. 11) the temperature dependence of the spectra is reversed in comparison with that in Fig. 10. But each of these types of temperature dependence mentioned above has been found already by the examination of other azocoupling products. Thus, e.g., the dependence illustrated in Fig. 11 is entirely similar to that found for other azocoupling products in cyclohexanone [20], formamide [21] or water [25a], while the reversed dependence from Fig. 10 is similar to that of 1-phenylazo-4-naphthol in ethanol [17b,29]. However, with an exception [20], the proposed equilibrium for each of the above cited temperature dependence has been the azo–hydrazone equilibrium. Therefore, it may not be excluded the possibility of the involvement, beside the acid–base equilibrium $3b \rightleftharpoons 1a$ (Fig. 11), of the azo–hydrazone equilibrium $1a \rightleftharpoons 1b$ (Fig. 10) in the temperature dependence of spectra of **1** in ethanol (see also the final discussion from Section 2.2.4).

Anyway it is to underline that the absorption curves at different temperatures present isosbestic points and the fact that the observed changes with temperature increase are completely reversible by cooling to the initial temperature.

2.2.6. The time dependence of the UV–vis spectra of **1** in absolute ethanol

Although the time dependence of the spectrum of **1** in ethanol is irregular (Figs. 12 and 13) apparently are present two species in equilibrium because the absorption curves at different registration time intervals, after the preparation of the solution, show a quite well-defined isosbestic point (Fig. 12). But the equilibrium position seems to oscillate with time (Fig. 12) similar to the variation of the absorbance at a certain wavelength (Fig. 13). At the beginning the equilibrium shifts towards the species with the absorption bands at lower wavelength (about 435 and 395 nm) then, on the contrary, towards that with absorption band at longest wavelength in visible (over 520 nm), then again towards that of the lower wavelength and finally towards that with longest wavelength band – which we have assigned already to the hydrazone tautomer **1a**. The last shift continues, even if not with the same intensity, practically for a month, with only two insignificant opposite shifts at ~12 and 17 days (Fig. 13), respectively.

On the other hand, the absorption curves at different registration time intervals of **1** in ethanol (Fig. 12) are similar to those from Figs. 8 and 10 that have been shown above (Sections 2.2.3 and 2.2.5) to correspond apparently to acid–base equilibrium **1a** \rightleftharpoons **3b**. Therefore, we consider that also the equilibrium which is exhibited when investigating the time dependence of the spectra of **1** in ethanol (Fig. 12) corresponds firstly to the acid–base equilibrium **1a** \rightleftharpoons **3b**. The irregular variation of the position of this with the time is caused probably

by the complex interaction of the involved species (the hydrazone **1a** and the anion **3b**) with ethanol used as solvent. These complex – and different – solvent–solute interactions should be of the type involved by the solvation (ion–dipole, hydrogen bonding and dipole–dipole interactions) and probably these evolves more or less at hazard especially in the first time interval after dissolving (dissolution). It is possible that this evolution be bound to the low solubility of the dye **1**. We mention that such a time dependence of the spectra of the azocoupling products was investigated rarely (e.g. [27a,32]) and in each case this dependence has shown a certain irregularity. But the other authors [27a] have ascribed such a time dependence of the spectra to an unexpected manner of the interconnection of the azo–hydrazone – and dimerization- equilibria. It is appreciated [27a] that a certain concentration increase determines an aggregation of the azomonomer whilst the further concentration increase determines the disaggregation to the hydrazone monomer of the previously aggregate. Evidently the possibility of superimposition of such equilibria upon the acid–base one **1a** \rightleftharpoons **3b** cannot be excluded (compare also Sections 2.2.4 and 2.2.5) but now we have no clear argument for these. We hope that further investigation in this direction will bring more light.

2.3. Conclusions

The pH-dependence of the UV–vis absorption spectra of the aqueous ethanol solutions of the dye **1** indicates three interconnected acid–base equilibria (**2b** \rightleftharpoons **1a** \rightleftharpoons **3b** \rightleftharpoons **4b**) that have been characterized by the corresponding pK_a' values. There were also ascribed the four involved species (**1a**, **2b**, **3b**, **4b**). The hydrazone structure **1a** of the initial species is supported also by the ^1H and ^{13}C NMR data.

The dependence of the UV–vis spectra of the (aqueous) ethanol solution of **1** on the water content, dye concentration, temperature or time has been interpreted as being determined firstly by the manifestation in the examined conditions of the acid–base equilibrium **1a** \rightleftharpoons **3b**. However, due to some irregularities found at the above investigations there is not totally excluded the possibility of the superimposition upon the acid–base equilibrium **1a** \rightleftharpoons **3b** of the azo–hydrazone (e.g. **1a** \rightleftharpoons **1b**) and/or aggregation equilibria. Anyway, the great sensitivity to experimental factors of the UV–vis spectra of (aqueous) ethanol solutions of **1** is caused firstly by acid–base equilibria.

3. Experimental

The synthesis and purification of the dye **1** were made as previously described [1–3] (cf. [30]). Analytical grade reagents and solvents were provided by Merck (Darmstadt), Fluka (Bucks), Primexchim and Cristal (Bucharest). They were used without further purification. The water used was doubly distilled. As a rule a relatively concentrated (10^{-4} – 10^{-5} mol L $^{-1}$) stock solution of the dye **1** in ethanol was prepared. This solution was used as such or diluted with initial solvent or water or HCl or KOH solution to the concentration needed in spectroscopic measurements (10^{-5} – 10^{-6} mol L $^{-1}$).

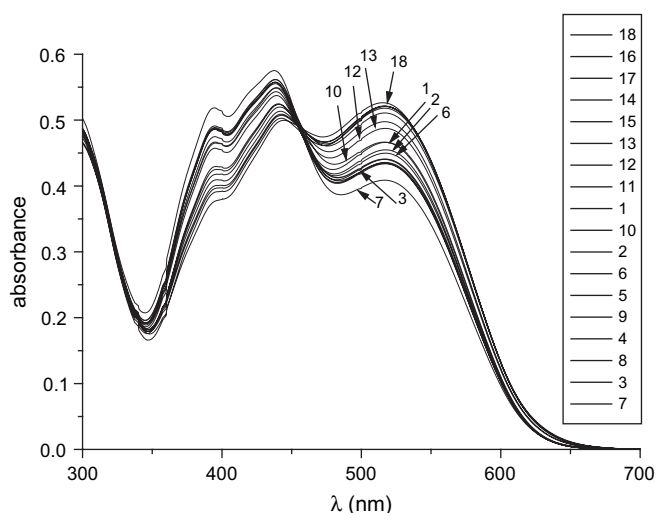


Fig. 12. The time dependence of the spectra of ethanol solution of **1** ($c = 3.44 \times 10^{-5}$ mol L $^{-1}$). For each curve is given the time interval in hours that is gone from the preparation of the solution up to the registration of the spectrum. 1 – 0 (the initial probe); 2 – 0.36; 3 – 1.26; 4 – 2; 5 – 2.83; 6 – 3.36; 7 – 20.3; 8 – 52; 9 – 70.5; 10 – 118; 11 – 142; 12 – 166; 13 – 191; 14 – 291; 15 – 337; 16 – 410; 17 – 480; 18 – 678.

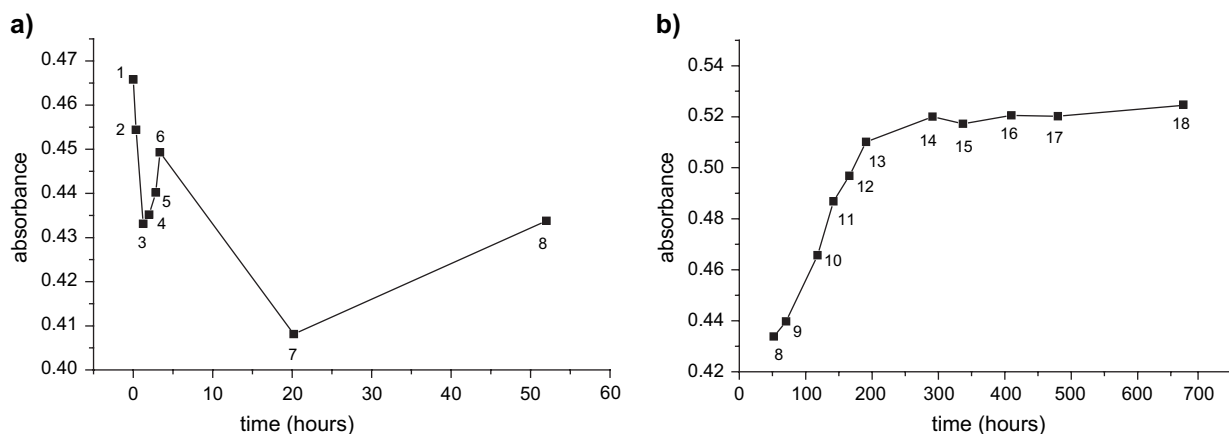


Fig. 13. The plot absorbance at 520 nm vs. time for ethanol solution of **1** ($c = 3.44 \times 10^{-5} \text{ mol L}^{-1}$) at room temperature. Each point corresponds to a time interval that is gone from the preparation of the solution up to the registration of the spectrum. (a) The first 52 h; (b) from 52 to 678 h.

The ionization constants (pK_a' values) were determined at 25°C in the presence of 0.01 mol L^{-1} KCl on the basis of correlation between pH' and absorbance at analytical wavelength (520 nm). The correlation was fitted with the aid of the programme *Table Curve Windows* v.1.10, *Table Curve*TM, Jandel Scientific, Copyright 1989–1993 AISN Software. The pH' of solutions was established by the addition of either HCl or KOH with the object to discourage dye aggregation (cf. [26a]). The electronic absorption spectra were performed on a *Jasco-V-520 spectrophotometer*. Matched glass or quartz cells of 0.5, 1.0, 2.0 and 5 cm were used. Especially by the examination of temperature- or time-dependence the cells have been tightly closed during the entire measurement. The experimental pH' values corresponding to the working conditions were measured by a digital *Pracitronic MV-870 pH-meter* equipped with a combined pH-reference electrode ESHC-02, produced by Naposenz SRL, Cluj Napoca. Because the pH' and pK_a' values were measured in (aqueous) ethanol solutions for these are used the pH' and pK_a' notations. The temperature was controlled with an ultra thermostat. The NMR spectra were registered in CDCl_3 with a Varian Gemini 300 (300 MHz) spectrometer.

Acknowledgement

The financial support for the study by the Romanian National University Research Council (CNCSIS grant A-131/2004) is gratefully acknowledged by authors.

References

- [1] Bâldea I, Ghirişan A, Panea I. *J Chem Soc Perkin Trans 2* 1992;1715–9.
- [2] Panea I, Ghirişan A, Cristea I, Gropeanu R. *Rom Pat* 114.797 C1; 1999.
- [3] Panea I, Ghirişan A, Bâldea I, Silaghi-Dumitrescu I, Crăciun L, Silberg IA. *Studia Univ “Babeş-Bolyai” Chemia* 2003;48(2):67–83.
- [4] Elguero J, Marzin C, Katritzky AR, Linda P. *The tautomerism of heterocycles*. New York: Academic Press; 1976. p. 336–9.
- [5] (a) Hinsche G, Uhleman E, Zeigan D, Engelhardt G. *Z Chem* 1981;21: 414–5;
- (b) Zeigan D, Kleinpeter E, Wilde H, Mann G. *J Prakt Chem* 1981;323: 188–98.
- [6] Kuzmina LG, Grigoreva LP, Strudika IuT. *Khim Geterosikl Soedin* 1985;815–21.
- [7] Mustroph H. *Z Chem* 1987;27:281–9.
- [8] Lyca A, Mustroph H. *J Prakt Chem* 1989;311:11–4.
- [9] El-Haty MT. *Asian J Chem* 1991;3:189–96.
- [10] Nikiforov EV, Zaitsev BE, Sheban GV, Riabov MA, Abramenco PI. *Zh Obshch Khim* 1992;62:1135–40.
- [11] Whitaker A. *J Soc Dyers Color* 1995;111:66–72.
- [12] Lyca A. *Dyes Pigments* 1999;43:27–32.
- [13] Bâtiu C, Panea I, Ghizdavu L, David L, Ghizdavu Pellascio S. *J Therm Anal Color* 2005;79:129–34.
- [14] Balderas-Hernandez P, Ramirez MT, Rojas-Hernandez A, Gutierrez A. *Talanta* 1998;46:1439–52.
- [15] Smith SA, Pretorius WA. *Water SA* 2002;28:395–402.
- [16] Abd-Allah EM, Rageh NM, Salman HMA. *J Chem Eng Data* 2003;48: 652–6.
- [17] (a) Burawoy A, Salem AG, Thompson AR. *J Chem Soc* 1952;4793–8. *J Chem Soc* 1953;1443–7;
- (b) Fischer E, Frei YE. *J Chem Soc* 1959;3159–63.
- [18] Zollinger H. *Azo and diazochemistry*. New York: Interscience; 1961. p. 323–37.
- [19] (a) Reeves RL, Kaiser RS. *J Org Chem* 1970;35:3670–5;
- (b) Nepras M, Titz T, Necas M, Lunak S, Hrdina R, Lyca A. *Collect Czech Chem Commun* 1988;53:213–26.
- [20] Peng Q, Li M, Gao K, Cheng L. *Dyes Pigments* 1991;15:263–74. 1992;18:271–86.
- [21] (a) Stoyanov St, Antonov L. *Dyes Pigments* 1988;10:33–45;
- (b) Antonov L, Stoyanov St. *Anal Chim Acta* 1995;314:225–32.
- [22] Ibanez GA, Olivieri AC, Escandar GM. *J Chem Soc Faraday Trans* 1997;93:545–51.
- [23] Rageh NM. *J Chem Eng Data* 1998;43:373–7.
- [24] Coe LdlC, Cardwell TJ, Catrall RW, Kolev SD. *Anal Chim Acta* 1998; 360:153–9.
- [25] (a) Iijima T, Jojima E, Antonov L, Stoyanov St, Stoyanova T. *Dyes Pigments* 1998;37:81–92;
- (b) Monahan AR, Germano NJ, Blossey DF. *J Phys Chem* 1971;75: 1227–33.
- [26] (a) Oakes J, Gratton P. *J Chem Soc Perkin Trans 2* 1998;1857–64. 2563–8;
- (b) Oakes J, Gratton P, Clark R, Wilkes J. *J Chem Soc Perkin Trans 2* 1998;2569–75.
- [27] (a) Dakiky M, Kanan K, Khamis M. *Dyes Pigments* 1999;41:199–209;
- (b) Dakiky M, Nemcova I. *Dyes Pigments* 2000;44:181–93.
- [28] Ertan N. *Dyes Pigments* 2000;44:41–8.
- [29] Joshi H, Kamounah FS, Zwan van der G, Gooijer G, Antonov L. *J Chem Soc Perkin Trans 2* 2001;2303–8.

- [30] Panea I, Ghirişan A, Cristea I, Gropeanu R, Silberg IA. *Heterocycl Commun* 2001;7:563–70.
- [31] Panea I, Ghirişan A, Iura F, Gropeanu R, Silberg IA. *Studia Univ “Babes-Bolyai” Chemia* 2003;48(2):55–65.
- [32] Panea I, Pelea M, Silberg IA. *Dyes Pigments* 2006;68:165–76.
- [33] Silverstein RM, Bassler GC, Morrill TC. *Spectrometric identification of organic compounds*. 5th ed. New York: John Wiley and Sons; 1991. Table 5.9.
- [34] Cristea I, Panea I. *Studia Univ “Babes-Bolyai” Chemia* 1995;40(1–2): 171–6.
- [35] Raue R, Riester O. In: *Ullmanns Encyclopaedia der Technische Chemie*. 4th ed., vol. 16. Weinheim: Verlagchemie; 1978. p. 636, 637, 657–62.
- [36] Zollinger H. *Color chemistry*. 2nd ed. Basel: VCH; 1991; (a)p. 288–291;(b)p. 130–137.
- [37] Griffith J. *J Soc Dyers Color* 1972;88:106–9.
- [38] (a) Mustroph H. *J Prakt Chem* 1985;327:121–8; (b) Mustroph H, Potocnak J, Grossmann N. *J Prakt Chem* 1984;326:979–84.
- [39] (a) Bell SJ, Mazzola EP, Coxon B. *Dyes Pigments* 1989;11:93–9; (b) Bell SJ, Mazzola EP, Di Novi MJ, Reynolds WF, Nielsen KW. *J Heterocycl Chem* 1991;28:641–5.
- [40] Schreiber J, Kulic J, Panchartek J, Vecera M. *Collect Czech Chem Commun* 1971;36:3399–403.
- [41] Bates RG. *Electrometric pH determination*. London: John Wiley; 1954. p. 31–3, 62–3, 71–4, 108–12, 281.